High Temperature Oxidation Behavior of Aluminide Coating Fabricated on UNS S30815 Stainless Steel

M. Rabani [1], M. Zandrahimi *[2], H. Ebrahimifar [3]

[1, 2] Department of Metallurgy and Materials Science, Faculty of Engineering, Shahid Bahonar University of Kerman, Kerman, Iran

[3] Department of Materials Engineering, Faculty of Mechanical and Materials Engineering, Graduate University of Advanced Technology, Kerman 7631133131, Iran.

Abstract

Aluminide coatings are widely used as a protective coating material due to their high corrosion and oxidation resistance properties. In this research, an aluminide coating was fabricated through aluminizing on UNS S30815 austenitic stainless steel using pack cementation method at 950 °C for 5 h. The isothermal oxidation was exerted on uncoated and aluminide coated steels for 200 h at 1050 ºC. Also cyclic oxidation was applied for 50 cycles at 1050 ºC on coated and uncoated steels. Surface morphology and cross section of coated and oxidized samples were characterized by means of scanning electron microscopy (SEM) and energy dispersive X-ray spectrometry (EDS). X-Ray diffraction (XRD) was used to identify the formed phases in the surface layer of as-coated and oxidized specimens. As-coated UNS S30815 consisted of Al_5Fe_2, $FeAl_3$ and Al_2O_3 phases. The results of the isothermal oxidation showed that the coated steel had lower weight gain (2.9 $mg.cm^{-2}$) after 200 h of oxidation in comparison with uncoated one (7 $mg.cm^{-2}$). Also the results of cyclic oxidation showed that the coated specimens had good resistance to thermal cycles.

Keywords: UNS S30815 austenitic stainless steel; Aluminizing; Pack Cementation; Oxidation.

1. Introduction

Heat-resistant austenitic stainless steels such as UNS S30815 are progressively used in petroleum, chemical, nuclear and other applications due to their good performance in high temperature oxidation environments and their relatively low price [1, 2]. Protection at high temperatures is subsequently conferred through the development of their respective oxides. Oxidation resistance of these stainless steels is due to the formation of Cr_2O_3 on the surface. The Cr_2O_3 is good for oxidation protection up to about 1000 °C but above this temperature the protection capability deteriorates rapidly [3].

One approach to overcome these problems is through the application of a protective coating on the stainless steels such as intermetallic compounds. Intermetallic, such as FeAl, $FeAl_2$, Fe_2Al_3, Fe_2Al_5 and $FeAl_3$, and FeAl are unique materials owing to their excellent high temperature oxidation and corrosion properties [2-5].This combination of useful properties makes them very attractive as high-temperature structural materials for aerospace, automotive and other applications [6-8].

Diffusion aluminide coatings in which protection

**Corresponding author*
E-mail: m.zandrahimi@uk.ac.ir
Address: Department of Metallurgy and Materials Science, Faculty of Engineering, Shahid Bahonar University of Kerman, Jomhoori Eslami Blvd., Kerman, Iran.
1. M.Sc. Student
2. Professor
3. Assistant Professor

condition is provided by forming an adherent and slow growing layer of Al_2O_3 are widely used to protect steels against aggressive environment [3, 9]. Indeed, this layer can provide a good diffusion barrier to withstand high temperature oxidation and therefore, increase their life time in aggressive atmospheres.

Numerous methods exist for applying aluminide coatings such as, CVD and PVD methods, pack cementation, thermal spray, magnetron sputtering, laser cladding and plasma spraying. Among these, pack cementation is an effective and inexpensive method [10, 11]. Pack cementation is a relatively simple technique, which consists of the coating element source, an activator, which is usually a halide salt, and an inert filler material, most often alumina to prevent the source from sintering at high temperature [12- 15].

Xiang et al. [16, 17] aluminized low carbon steel by pack cementation at the temperature range of 600 to 750 °C. The coating was a single layer of Fe_2Al_5 or $Fe_{14}Al_{86}$ phase with an activation energy of about 75 kJ/mol. Ei-Mahallawy et al. [18] carried out hot-dip aluminizing on low carbon steel in a pure aluminum bath with an activation energy of 138 kJ/mol. The coating comprised $FeAl_3$, Fe_2Al_5 and $FeAl_2$ phases.

In another research the aluminide coating was prepared on Ti-6Al-2Zr-1Mo-1 V titanium alloy by pack cementation to enhance the high temperature oxidation resistance for aircraft and aerospace applications.

The excellent oxidation resistance performance was attributed to the formation of a continuous and dense Al_2O_3 layer on the TiAl3 coating surface, which was effective to prevent the O element diffusing into the coating and then reduce the oxidation rate [19].

Also in another research an Al-Ti coating was deposited onto the martensitic steel by pack cementation technique. Formation of α-Al_2O_3/TiO_2/transition layer beneath the oxide scale decreased oxygen transport into the coating significantly [20].

According to our survey of literatures, no research has been done on the coating of aluminum on UNS S30815 stainless steel using pack cementation method for the application of high temperature devices.

The present research aims to evaluate the oxidation aluminide coated UNS S30815 Stainless steels coated using pack cementation method. To evaluate oxidation behavior, different types of oxidation, such as isothermal oxidation and cyclic oxidation at 1050 °C were carried out to investigate the role of the coating layer during oxidation.

2. Experimental Procedure

2. 1. Substrate preparation

In this investigation, aluminization of UNS S30815 stainless steel was carried out by employing the halide-activated pack cementation process. The composition of the type UNS S30815 stainless steel used in this report is shown in Table 1. Before coating process, the substrates were polished from 400-grit SiC paper up to 1200-grit. After polishing, samples were cleaned in ultrasonic bath with acetone for 1 min.

2. 2. Coating process

To create aluminum coating on UNS S30815 stainless steel, pack cementation was employed. This process included the use of a pack mixture in a horizontal argon furnace with a constant temperature zone of about 100 mm length.

Fig. 1 demonstrates a schematic diagram of the pack cementation device employed to make the coatings.

The samples were immersed in a pack of powder mixture of 10 wt.% Al (325 mesh), 3 wt. % NH_4Cl (activator) and 87 wt. % Al_2O_3 (inert filler, 325 mesh). Among the chloride salt, NH_4Cl is a very effective

Table 1. Chemical composition of UNS S30815 Stainless steel wt. %.

steel	Composition (wt. %)										
	Fe	C	Cr	Ni	Si	Mn	N	Ce	P	S	Ti
UNS S30815	Bal.	0.08	21.4	11.8	1.9	0.4	0.15	0.04	0.03	0.02	-

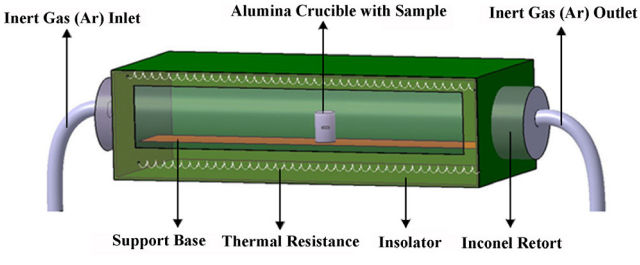

Fig. 1. Schematic diagram of the pack cementation device.

activator [15]. The substrate samples and pack materials were placed in an austenitic stainless steel crucible, closed with an austenitic stainless steel lid. To remove moisture from the pack, the crucible was placed into an electric tube furnace heated to 200 ºC and held at this temperature for 2 h. The furnace was circulated with argon, and the temperature was raised to 950and held there for 5h. The furnace was then cooled to room temperature at its natural rate by switching off the power supply while maintaining the argon gas flow. After pack cementation, the crucible was taken out of the furnace, the lid was removed, and the coated samples were discharged from the pack and were ultrasonically cleaned in ethanol to remove any embedded pack material.

2. 3. Oxidation tests

Based on the application of stainless steels at high temperatures such as boilers and nuclear industries, isothermal oxidation test was carried out at 1050 ºC for 200 hours. Also, cyclic oxidation test at 1050 ºC for 50 cycles was used to evaluate the resistance of coated stainless steel against thermal stresses [2, 13].

The isothermal oxidation tests of the coated samples were carried out in air in an electrical furnace at 1050 ºC. For thermal cycling test, the coated samples were kept for 10 min in furnace in air at 1050 ºC and for 10 min in room temperature alternatively for 50 times. For the oxidation tests, two groups of samples were used: bare specimens and coated specimens. Mass changes of the oxidized specimens were measured after fixed time intervals using a balance with 0.1 mg sensitivity. Three parallel samples were adopted for acquiring average mass change during the thermal exposure.

2. 4. Microstructural characterization

The microstructure and chemical composition of cross-sections of the coated specimens were analyzed using scanning electron microscopy (SEM) (CamScan MV320) with energy dispersive spectroscopy (EDS). The working distance of the samples from the tip of the electron gun and the accelerating voltage were adjusted to 23 mm and 20 kV, respectively. The different phases of the surface layers were determined with an X-ray diffraction (XRD) technique. A Philips X'Pert High Score diffractometer was used with Cu Kα radiation (=1.5405 A), a step angle of 0.02° and time step of 1 sec/degree in all the measurements.

3. Results and Discussion

3. 1. Aluminizing

Microstructure of the coating obtained from the pack cementation method is shown in Fig. 2. As can be seen, the total thickness of the coating is about 350 µm (Fig. 2a). This figure shows that the coated layer can be sub-divided into 3 layers; an outer Al enriched layer with the approximate thickness of 180±7 µm and a middle layer with the approximate thickness of 110±8 µm and an inner 60±3 µm thick. There are no cracks and distinct inter diffusion zones or large holes observed in the coating and the interface of coating and substrate.

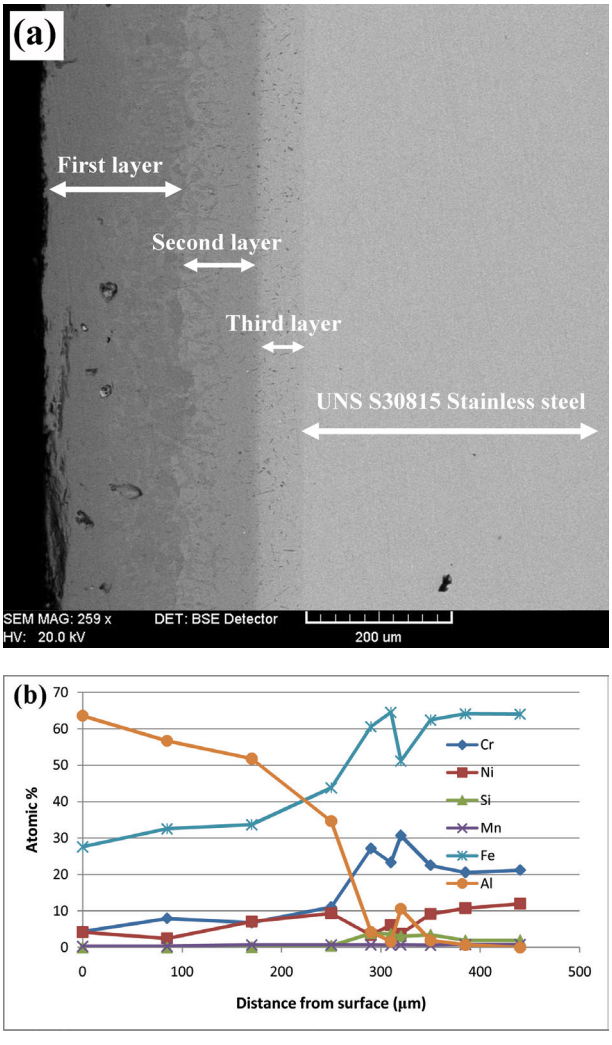

Fig. 2. SEM cross-sectional micrograph of aluminized sample (a) and EDS results showing the concentration variations of Cr, Ni, Si, Mn, Fe, and Al elements near the surface of the aluminized UNS S30815 Stainless steel (b).

The concentration profiles measured by the EDS analyzer revealed a three-layer phase structure across the thickness of the coating layer (Fig. 2b). The Al concentration at the edge of the first layer was about 65 wt. %. Such a high Al content can lead to good oxidation and hot corrosion resistance [21], also it shows a low amount of Al diffused into the steel and the contents of Fe, Cr and Ni are diluted in the coating by the incoming Al.

Fig. 3 shows the X-ray diffraction pattern of the surface of the aluminized sample. The diffraction pattern

indicates the formation of Al_5Fe_2, $FeAl_3$ and Al_2O_3. Although the substrate is austenitic stainless steel, its characteristic peaks are absent, indicating that a rather thick aluminized layer was formed.

According to EDX analysis of the cross-section of the coating as well as XRD analysis, the first layer structure which is rich in aluminum consists of Al_5Fe_2. Due to the high intensity of the Al_5Fe_2 phase peak, this phase is dominant in the first layer and $FeAl_3$ phase was formed by the reduction of aluminum. There is also some Al_2O_3 phase on the surface of the first layer due to the powder mixture attached to the surface of the first layer. In the second and third layers according to EDX analysis and reduction of the aluminum content the dominant phase in these layers contains Al_5Fe_2.

Theoretically, $FeAl_3$ phase has the lowest free energy of formation among all the Al–Fe compounds in the Al–Fe system [4] and therefore the formation of this compound is expected preferentially. However, the formation of Al_5Fe_2 phase in most cases is due to the highest growth rate and favored crystallographic orientation (c axis) [22].

The presence of Al_2O_3 is believed to be the residual filler material remained after cleaning [1]. There are fewer phases observed than in the binary Fe-Al phase diagram, which might be due to problems with nucleation and growth in most of the phases [3]. In addition, based on the Fe-Al equilibrium phase diagram [4], Fe_2Al_5 and $FeAl_3$ phases form at higher amounts of Al [23]. This result indicates that Fe_2Al_5 is the main phase in the coating, consistent with the previous works for high activity pack cementation [10, 24].

Behador and his co-workers studied the deposition of Al into steel by pack-cementation method [25]. They illustrated that the creation of Al alloys within the coating diffusion scope began approximately from 480 ºC. The formation of alloys occurred quickly within the diffusion coating temperature range based on the equilibrium phase diagram of Fe-Al [4] and the alloy layer included one or several phases consisted of FeAl, Fe_3Al, Fe_2Al_3, $FeAl_2$, Fe_2Al_5 and $FelAl_3$.

Fundamentally, the coating created in a high-activity powder mixture contains the $FeAl_3$ phase, but an activity with low char resulted in the creation of FeAl, Fe_3Al and normally a surface layer of alumina [10]. Therefore, it could be deduced that the presence of $FeAl_3$, Fe_2Al_5 and Al_2O_3 in the coating discloses the activity with a high char accompanied by the inward diffusion of coating elements.

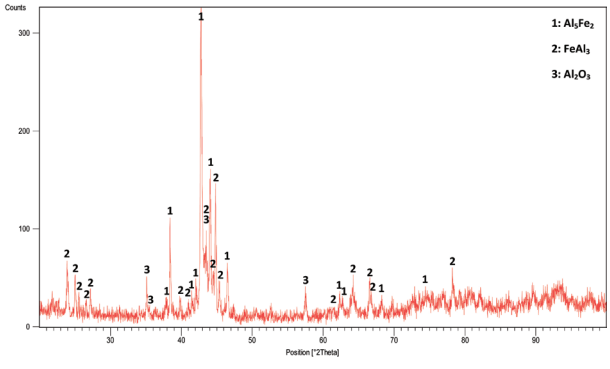

Fig. 3. XRD analysis of aluminized sample.

3. 2. Isothermal oxidation

The samples were put inside or taken out of the furnace directly to air within several seconds. After cooling from 1050 ºC to room temperature, the samples were weighted by an electronic balance with a sensitivity of 0.1 mg. Weight change percentages (W%) of the samples were calculated by the Eq. (1):

$$\Delta W\% = \left(\frac{m0 - m1}{m0}\right) \times 100\% \qquad \text{Eq. (1)}$$

, where m_0 and m_1 are the weight of the samples before oxidation and after oxidation, respectively. Fig. 4a shows the isothermal oxidation weight change of bare and aluminized UNS S30815 specimens at 1050 ºC in static air.

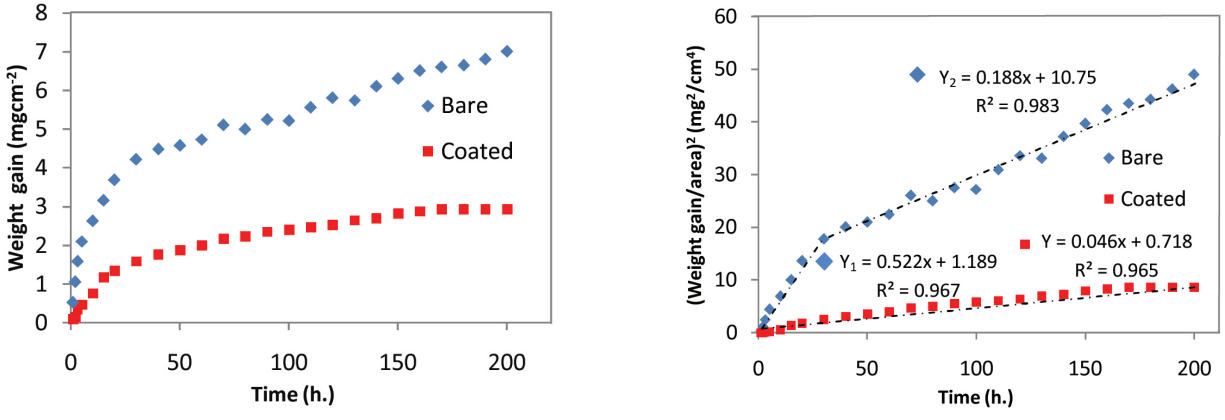

Fig 4. Mass gain of alloy during isothermal oxidation in air at 1050 for 200 h: (a) mass gain versus time; (b) square of mass gain versus time. oxidation for coated and uncoated samples.

At this temperature, the uncoated samples show a significant weight gain at initial stage up to 40 h, and follow an obvious weight loss after 40 h. At this temperature, the weight loss of uncoated specimen is remarkable. This means that the UNS S30815 cannot possess oxidation resistance at 1050 ºC due to the volatilization of chromium oxide [3, 26]. However, for aluminized specimens, the kinetics of the isothermal oxidation follows the parabolic rate law even during oxidation at 1050 ºC, indicating that oxide scales formed on the surface of aluminized coatings can act as a diffusion barrier to suppress the transport of oxygen and cations. The total oxidation weight gains after 200 h of oxidation in air at 1050 ºC for coated substrate was 2.9 mg cm^{-2}, which is smaller than that of the uncoated one (7 mg cm^{-2}). From the weight gain result, it is evident that the coated specimens showed better oxidation resistance. Fe–Al intermetallic phases such as Fe_2Al_5 and $FeAl_3$ by higher aluminum content significantly enhanced the high temperature oxidation resistance [11, 27].

Fig. 4b shows a plot of square of weight-gain versus the time at 1050 in air time for oxidized bare and coated steel samples. The oxidation rate of uncoated and coated steels is shown in Table 2. In both samples, the weight gains increased parabolically with the isothermal oxidation time, satisfying the low parabolic kinetics described by:

$$(\frac{\Delta W}{A})2=kpt \qquad \text{Eq. (2)}$$

, where is the weight change (mg), A is the sample surface area (mm^2), t is the oxidation time (h) and kp is the parabolic rate constant in mg^2 cm^{-4} h^{-1}. It can be found that the square of mass gains of the blank and coating specimens were all nearly linear to the oxidation time. However, compared with that of the blank, the mass gains of coating specimens decreased significantly.

kp for the coated substrate was 6.41×10^{-14} $g^2cm^{-4}s^{-1}$ after 200 h oxidation, which is lower than that of the uncoated substrate (kp,1 = 3.6965 × 10−12 $g^2cm^{-4}s^{-1}$ between 0 and 40 h and kp,2 = 3.27×10^{-13} $g^2cm^{-4}s^{-1}$ between 40 and 200 h). Different values for kp of uncoated specimens at 0 to 40 h and 40 to 200 h were given because of the higher initial oxidation rate, which then decreased due to the stability of oxide scales [6].

It can be seen that, during the entire oxidation test, the parabolic rate constant for the oxidation of the coating specimen was lower than that of the bare which demonstrated that the coating specimen possesses excellent oxidation resistance.

Fig. 5 demonstrates the XRD analysis of surface of the uncoated and coated steels oxidized at 1050 ºC for 200 hours. In the XRD pattern of the uncoated samples (Fig. 5a) phases of Cr_2O_3, Fe_2O_3, and FeO are seen.

The formation of chromia refers to the outward diffusion of chromium and inward diffusion of oxygen. The creation of iron oxides is due to the outward diffusion of iron cations and inward diffusion of oxygen anion [15, 28].

Fig. 5b shows the XRD analysis of the aluminized

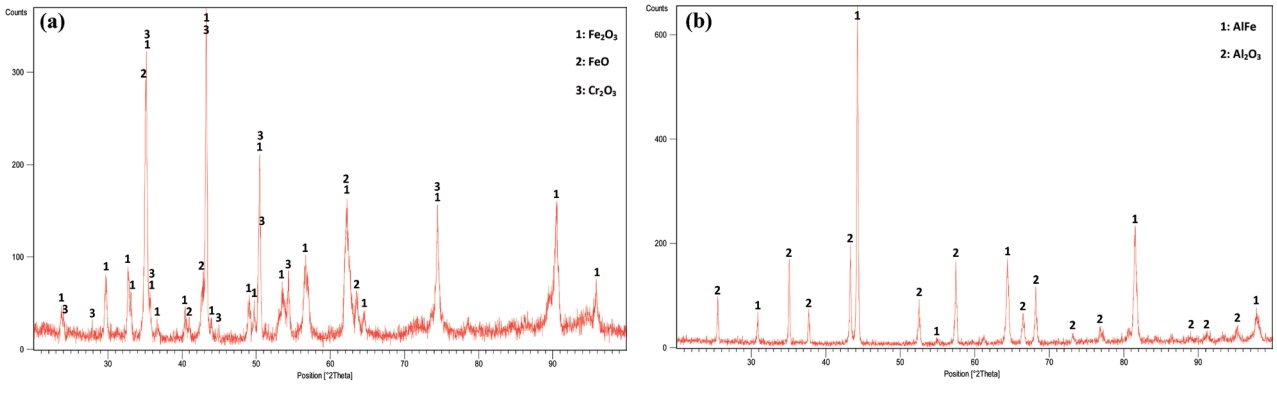

Fig. 5. XRD patterns of oxide scales formed on (a) bare and (b) aluminide coating after isothermal oxidation in air at 1050 ºC for 200 h.

Table 2. Isothermal oxidation rate constants (g^2 cm^{-4} s^{-1}) of aluminized samples and bare samples.

Processes	Parabolic rate constants
Aluminized samples	6.41×10^{-14}
Bare samples	3.6965×10^{-12} $g^2cm^{-4}s^{-1}$ (0 - 40 h),
	3.27×10^{-13} $g^2cm^{-4}s^{-1}$ (40 - 200 h)

specimen which is covered by Al_2O_3 and FeAl phases. During oxidation, Fe_2Al_5 and $FeAl_3$ phases converted to Al_2O_3 and FeAl phases [6, 13].

Fig. 6 shows SEM cross-section of uncoated (Fig. 6a) and coated sample (Fig. 6b) after 200 hours of oxidation at 1050ºC. For uncoated UNS S30815 (Fig. 6a), oxide layer and substrate are observed. The oxide scale layer approximately grew to ~ 380±20 µm. The total scale layer for the coated sample is ~ 420±12 µm. The initial thickness of the coating layer was 350 µm and reached 420 µm after 200 h of oxidation. The thickness of the oxide layer (Fe_2O_3+Cr_2O_3) grown in the coated sample is approximately 70 µm, which is much less than that of the uncoated sample (380 µm).

The results of Fig. 6 illustrate that in coated samples, the aluminized coating layer acts as an effective barrier against outward diffusion of Cr cations and inward diffusion of oxygen anions because it decreased the thickness of oxide layer (Fe_2O_3+Cr_2O_3) and also decreased the weight gain in coated substrates.

The oxide layer grown on the surface of the uncoated sample was porous and there were a large number of cracks on the surface while in the coated sample, the number of pores and cracks was very low and the adhesion of the coating layer to the substrate was very good after 200 h of isothermal oxidation. In the coated sample, there are a number of cavities in the interface between the oxide layer and the substrate. These cavities are due to the outward diffusion of the chromium cation and the formation of chromium oxide. Chromium oxide (Cr_2O_3) is a P type oxide growing through the penetration of chromium cations to the outside. Therefore, during the oxidation, vacant cations move inwards and by build-up in the oxide-metal interface, cause porosity and cavity in this region [7]. Another reason could be the difference between the thermal expansion coefficient of the oxide layer and the substrate.

The improved oxidation resistance of aluminized samples is due to the formation of Al_2O_3 on its surface. This result is in a good agreement with the result of our previous study [2]. It was reported that the AISI 304 alloy modified with Al and other alloying elements has better oxidation resistance at high temperatures than the bare samples.

The low oxidation resistance of the bare samples depends on Cr and the formation of Cr_2O_3 on its surface. Cr_2O_3 scale is capable to supply sufficient oxidation protection up to 1000 ºC and this oxide layer will be destabilized above 1000 ºC based on the Eq. (3) and will not protect the substrate against oxidation [3, 26].

$$Cr_2O_3\ (s) + 3/2O_2\ (g) = 2CrO_3\ (g). \qquad \text{Eq. (3)}$$

Therefore, Fe has been oxidized rapidly due to the lack of protective layer on the surface.

Fig. 7 shows SEM surface morphology of uncoated and coated samples after 200 hours of oxidation. The uncoated sample grew a black oxide scale, spalled from the surface in some areas (Fig. 7a). The created cracks in the surface of uncoated steel are likely concerned to stresses originated from differences in the thermal expansion coefficient (TEC) between the metallic substrate

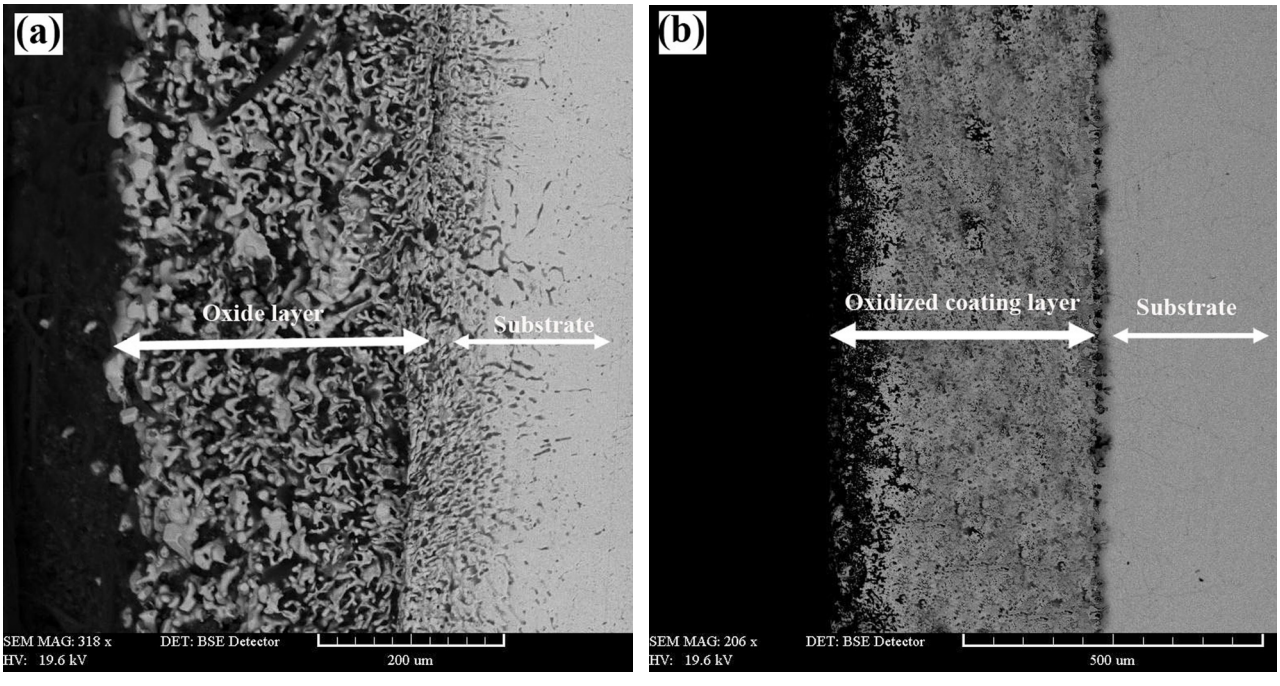

Fig. 6. SEM cross-section of uncoated (a) and coated sample (b) after 200 hours of isothermal oxidation at 1050 ºC.

and the formed oxides on the surface. TEC of iron oxides is larger than that of the stainless steel (10×10^{-6} ºC^{-1}) which results in tensile stresses in the oxide during cooling (FeO ~ 17×10^{-6} ºC^{-1}, Fe_3O_4 ~ 15×10^{-6} ºC^{-1}, Fe_2O_3=13×10^{-6} ºC^{-1}) [29].

Another reason for spallation and cracking in bare steels might be the formation of silica. Silica phase formation is related to steels with silicon higher than 0.5%. In such steels an insulating, continuous or network-like layer of silica can grow under the chromia scale [30, 31].

Silica is not miscible with chromia, and the poor adhesion between the oxides may cause detachment of chromia from silica. The poor adhesion between chromia and silica is due to the difference between the thermal expansion coefficients (TEC). The TEC of SiO_2 (0.55×10^{-6} ºC^{-1}) is remarkably lower than the TEC value of Cr_2O_3 (9.6×10^{-6} ºC^{-1}) [27,28]. Austenitic stainless steel has a TEC of ~ 10×10^{-6} ºC^{-1}, which is relatively close to the TEC of chromia [31, 32].

Spalled scale creates diffusion paths for cations and anions and therefore through the easy migration of ions the oxide layer grows with higher rates [7, 30-32].

The color of the coated specimen surface before the experiment was silver like, but after 200 h of isothermal oxidization, the color of the coating turned to dark gray without spallation and cracking (Fig. 7b).

3. 3. Cyclic oxidation

Cyclic oxidation tests were performed to evaluate the stability of coating formed on UNS S30815 stainless steel under cyclic thermal stresses. For this test, two groups of samples were used: bare and coated samples. Cyclic oxidation tests of two aluminized specimens and two substrates were conducted at 1050 °C. Each cycle consisted of 60 min heating at 1050 °C and cooling in air for 15 min. Weight changes were measured every 4 cycles with a precision electronic balance with accuracy of 1×10^{-4} g.

Fig. 8a shows a plot of the weight change per unit area vs. number of cycles for the test performed in air at 1050 °C for 50 h. According to Fig. 8, the weight changes of aluminized specimens are lower than the bare specimens. With the isothermal oxidation at 1050 °C, the cyclic oxidation kinetic curves of both coated and bare samples followed parabolic rate law. The bare specimen oxidized at a very high rate. The

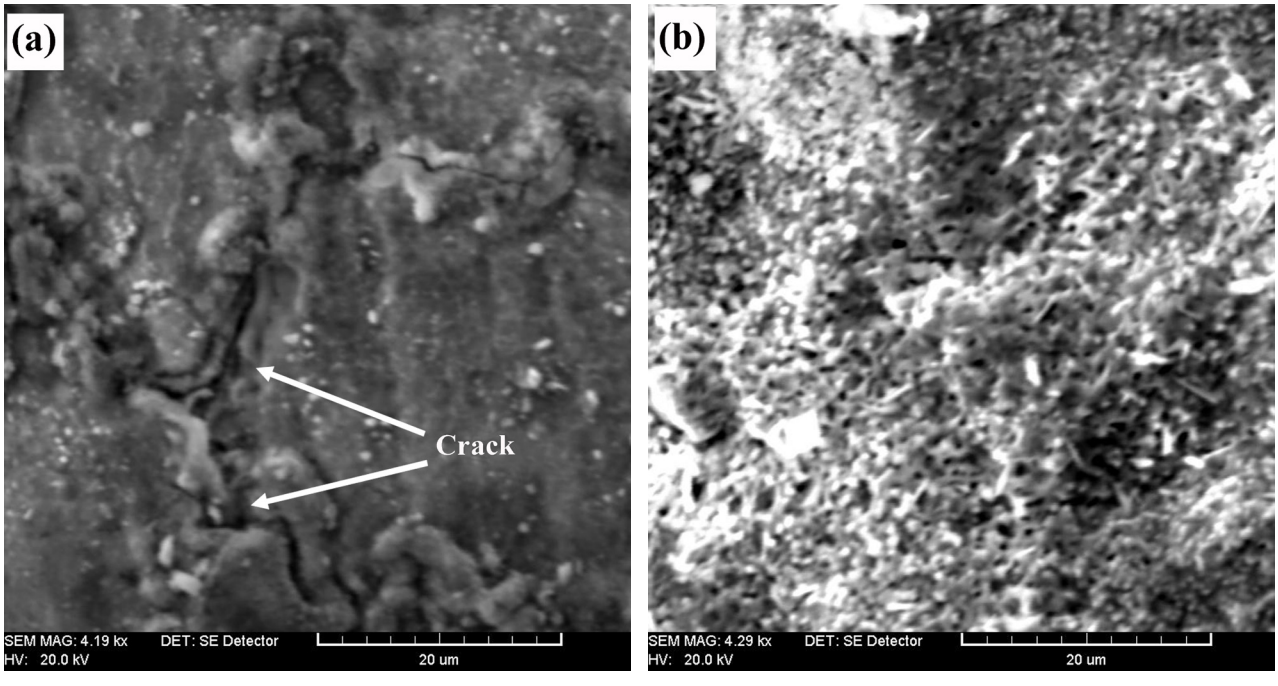

Fig. 7. SEM micrographs of (a) uncoated and (b) coated samples after 200 h isothermal oxidation at 1050 °C.

Table 3. Cyclic oxidation rate constants (g^2 cm^{-4} s^{-1}) of aluminized and bare samples.

Processes	Parabolic rate constants
Aluminized samples	3.46×10^{-13}
Blank samples	1.66×10^{-12} up to 25 cycle,
	2.22×10^{-11} from 25 cycle to 50 cycle

specimen deteriorated quickly and disintegrated into several pieces. The weight gain of uncoated specimen after 50 cycles was 7 mg/cm^2. The aluminide coating on UNS S30815 stainless steel exhibited the best overall oxidation resistance (by weight gain of 1.8 mg/cm^2).As shown in the enlarged plot for weight change in Fig. 8a, this specimen initially gained weight and showed only a little change in weight.

This specimen showed fairly good stability of the coating after 50 cycles. As indicated in Fig. 8b, the bare alloy exhibited a two stages oxidation kinetics (about 1.66×10-12 g^2.cm^{-4}. s^{-1} in the initial stage, and then it increases to 2.22×10^{-11} g^2.cm^{-4}. s^{-1}) which is much larger than that of the aluminized alloy (3.46×10^{-13}g^2.cm^{-4}. s^{-1}). The difference in the kp of bare steel may be obvious by the significant scale growth and thickening which occurred during the second stage (Table 3) [30-33].

Fig. 9 shows SEM images of the surface morphology, for the uncoated and coated specimens after the cyclic oxidation test. The uncoated specimen surface spalled from some areas (Fig. 9a), while the coated sample surface exhibited good resistance to spallation and cracking (Fig. 9b) after 50 cycles.

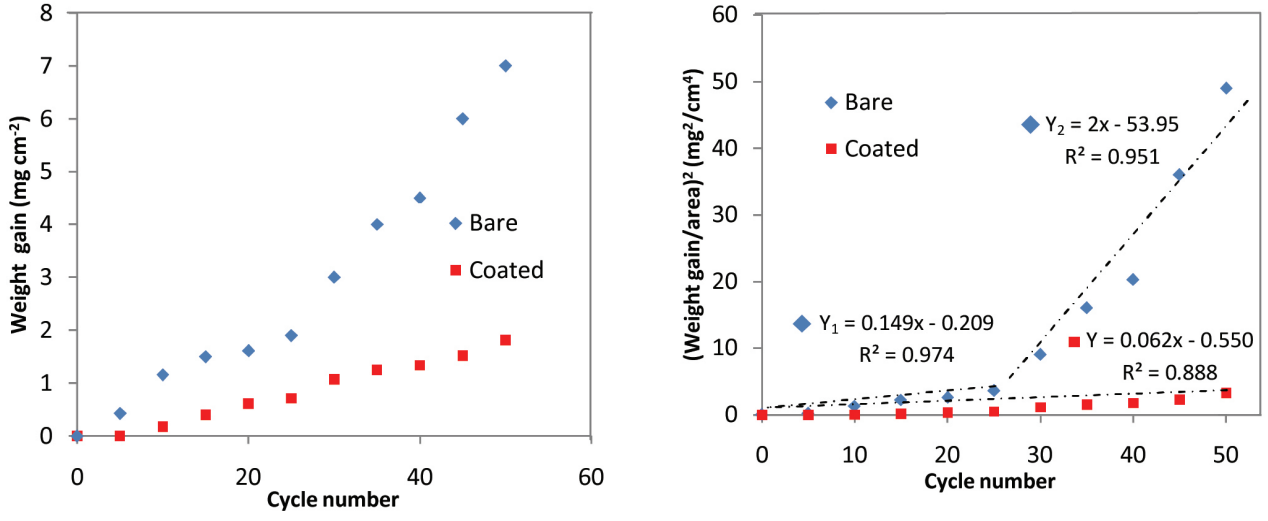

Fig. 8. Mass gain of alloy during cyclic oxidation in air at 1050 °C: (a) Mass gain versus time; (b) square of mass gain versus time.

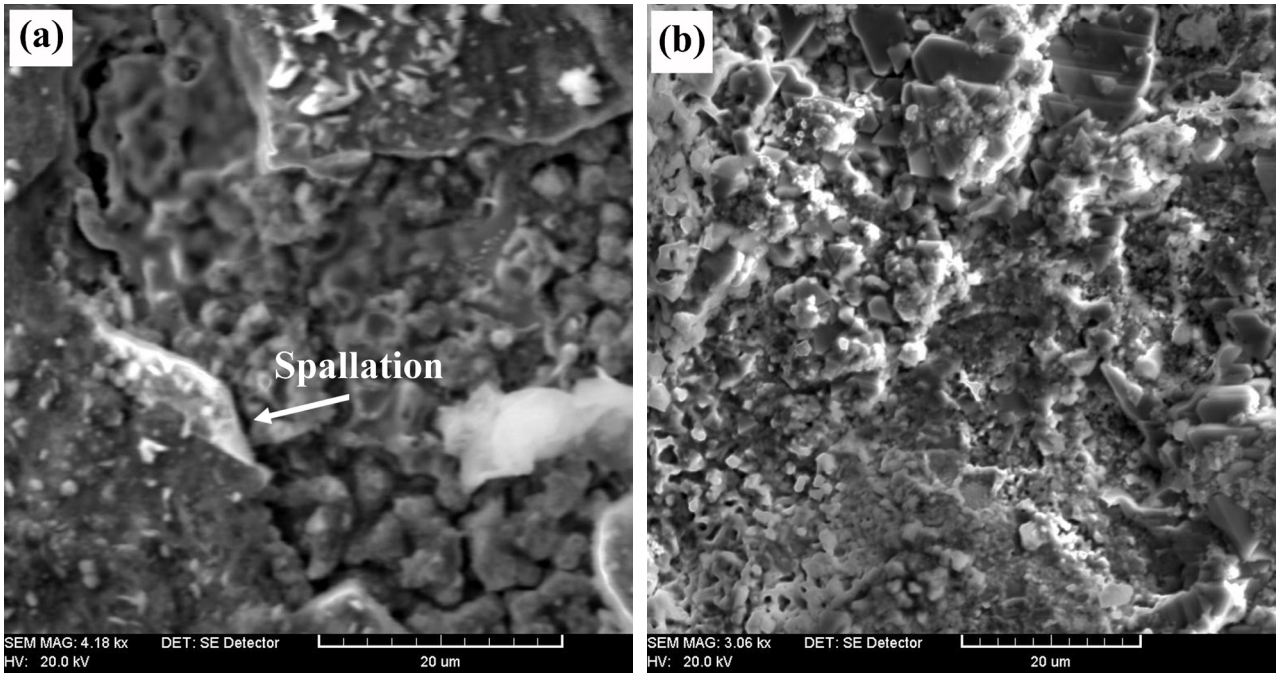

Fig. 9. SEM micrographs of (a) uncoated and (b) coated sample after 50 cycles at1050 °C.

Fig. 10 demonstrates SEM cross-section of uncoated (Fig. 10a) and coated sample (Fig. 10b) after 50 cycles of oxidation at 1050 ºC. For bare steel (Fig. 10a), oxide layer and substrate are distinguished. The thickness of grown oxide scale on the bare steel is approximately ~ 340±17 µm. The thickness of oxide scale for the aluminized sample is ~ 450±13 µm. The initial thickness of the aluminized layer was ~ 350 µm and reached 450 µm after 50 cycles of oxidation. The thickness of the oxide layer (Fe_2O_3+Cr_2O_3) grown in the aluminized sample is approximately 100 µm, which is much less than that of the bare steel (340 µm). In uncoated sample large spallation and cracks are observed (Fig. 10a) while in aluminized samples (Fig. 10b) the number of cracks and spallation is much lower.

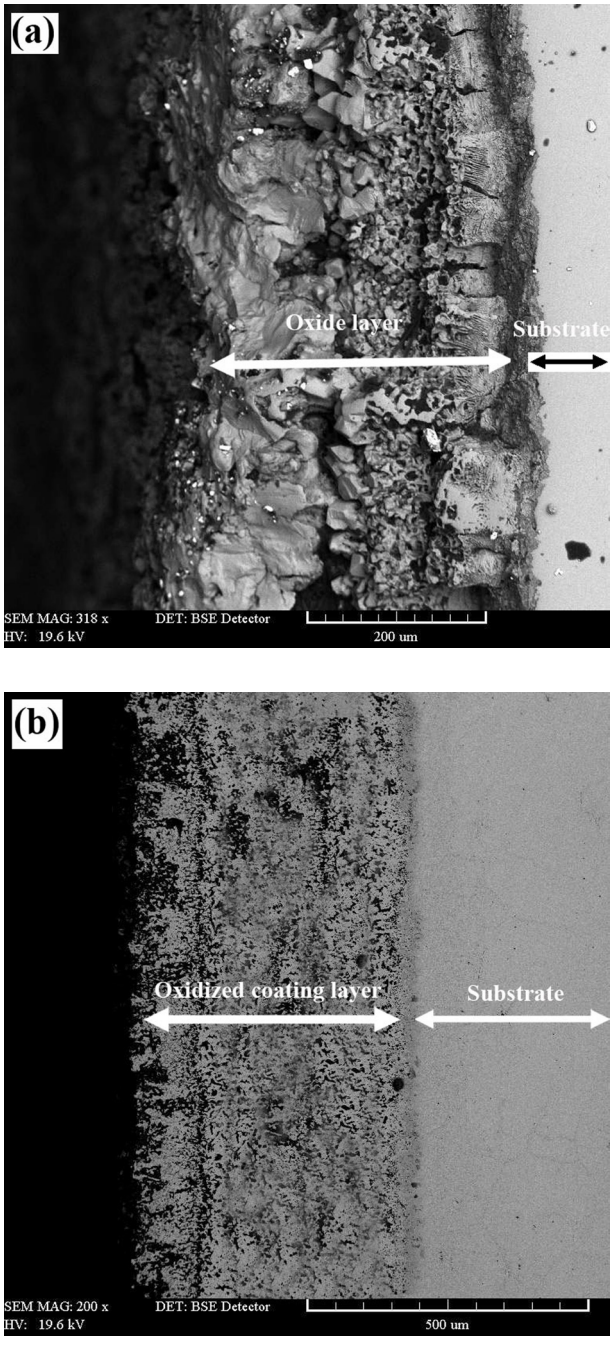

Fig. 10. SEM cross-section of uncoated (a) and coated sample (b) after 50 cycles of oxidation at 1050 ºC.

Oxide spallation or cracking during cyclic oxidation tests are due to the thermal stresses in the oxide scale. Thermal stresses arise due to the difference between the TECs of metallic alloy and the oxide scale [34, 35]. During heating, the oxide scale was subjected to tensile stresses which could be relieved by cracking. During cooling, high compressive thermal stresses were produced in the scale which might be release by spalling and cracking. Hematite formation beneath chromium oxide led to breakaway oxidation which resulted in cracking due to the thermal expansion coefficient mismatching of hematite and chromia.

Many factors such as maximum and minimum temperature, cooling and heating rate, cycle frequency and alloy composition affect the cyclic oxidation resistance of stainless steels [36]. Osgerby et al. [37] illustrated that the cooling hold time obviously affected the oxide resistance owing to the fact that fracture stresses are produced more quickly with cycles containing more cooling holds.

Another cause for spallation and cracking is the creation of cavities and pores at oxide scale/substrate interface. These defects during thermal stresses accumulate and produce the cracks. During the oxidation cracks grow and it results in the spallation. The cyclic oxidation test data shows that the aluminide coating on UNS S30815 stainless steel caused the improvement of cyclic oxidation resistance in comparison to the bare steel.

4. Conclusions

The aluminide coating on UNS S30815 austenitic stainless steel was produced through aluminizing by the use of pack cementation method. The following results was obtained:

- The aluminized layer consisted of three layers. The total thickness of the layers was about 350 m. The aluminized layer consisted of the Al_5Fe_2, $FeAl_3$, Al_2O_3 phases.
- The isothermal oxidation was performed at 1050 ºC for 200 hours. In both samples, the weight gains increased parabolically with the isothermal oxidation time confirming parabolic oxidation law. Results showed that the aluminized layer acted as a diffusional barrier against outward diffusion of chromium and inward diffusion of oxygen and resulted in the lower mass gain.
- The cyclic oxidation was done at 1050 ºC for 50 cycles. Results showed that the aluminized layer had good thermal expansion coefficient with stainless steel substrate and caused a superior oxidation resistance to spallation and cracking.

References

[1] W. T. Tsai and K. E. Huang: Thin Solid Films, 366(2000), 164.
[2] M. Zandrahimi, J. Vatandoost and H. Ebrahimifar: Oxid. Met., 76(2011), 347.
[3] S. Sharafi and M. Farhang, Surf. Coat. Tech., 200(2006), 5048.
[4] H. Baker, A. M. H. Volume, 03-Alloy Phase Diagrams, ASM International, (1992).
[5] O. Seri and M. Imaizumi: Corros. Sci., 30(1990), 1121.
[6] H. Ebrahimifar and M. Zandrahimi: Oxid. Met., 84(2015), 329.
[7] H. Ebrahimifar and M. Zandrahimi: Oxid. Met., 84(2015), 129.
[8] F. Üstel and S. Zeytin: Vacuum., 81(2006), 360.
[9] M. Bateni, S. Mirdamadi, F. Ashrafizadeh, J. Szpunar and R. Drew: Surf. Coat. Tech., 139(2001), 192.
[10] C. Houngninou, S. Chevalier and J. Larpin: Appl. Sur. Sci., 236(2004), 256.
[11] Y. Su, G. Hu, Z. Xu and J. Liu: Thermochim. Acta., 506(2010), 67.
[12] R. Bianco and R. A. Rapp: J. the Electrochem. Soc., 140(1993), 1181.
[13] M. Zandrahimi, J. Vatandoost and H. Ebrahimifar: J. Mater. Eng. Perform., 21(2012), 2074.
[14] S. Chakraborty, S. Banerjee, K. Singh, I. Sharma, A. Grover and A. Suri: J. Mater. Process. Tech., 207(2008), 240.
[15] H. Ebrahimifar and M. Zandrahimi: Oxid. Met., 75(2011), 125.
[16] Z. D. Xiang and P. K. Datta: Surf. Coat. Tech., 184(2004), 108.
[17] Z. D. Xiang and P. K. Datta: Acta Mater., 54(2006), 4453.
[18] N. A. Ei-Mahallawy, M. A. Taha, M. A. Shady, A. N. Attia and W. Reif: Mater. Sci.
Tech., 13 (1997), 832.
[19] H. Tian, K.Zhou, Y. C. Zou, H. Cai, Y. M. Wang, J. H. Ouyang and X. W. Li: Surf. Coat. Tech., 374(2019), 1051.
[20] Y. Wang, S. Feng, D. Liu, C. Zhang, J. Xu, C. Luo and J. Suo: Surf. Coat. Tech., 330 (2017), 277.
[21] S. -W. Mao, H.-L. Huang and D. Gan: Surf. Coat. Tech., 205(2010), 533.
[22] S. Guo, Z. Wang, L. Wang and K. Lu: Surf. Coat. Tech., 258(2014), 329.
[23] R. Dutta, S. Majumdar, A. Laik, K. Singh, U. Kulkarni, I. Sharma and G. Dey: Surf. Coat. Tech., 205(2011), 4720.
[24] Z. Zhan, Z. Liu, J. Liu, L. Li, Z. Li and P. Liao: Appl. Surf. Sci., 256(2010), 3874.
[25] A. Bahadur, T. Sharma, N. Parida, A. Mukherjee and O. Mohanty: J. Mater. Sci., 28(1993), 5375.
[26] Z. Zhan, Y. He, L. Li, H. Liu and Y. Dai: Surf. Coat. Tech., 203(2009), 2337.
[27] Z. Xiang and P. Datta: Surf. Coat. Tech., 184(2004), 108.
[28] L. Cooper, S. Benhaddad, A. Wood and D. Ivey: J. Power Sources., 184(2008), 220.
[29] M. Takeda, T. Onishi, S. Nakakubo and S. Fujimoto: Mater. Trans., 50(2009), 2242.
[30] H. Ebrahimifar and M. Zandrahimi: Oxid. Met., 84(2015), 329.
[31] S. Fontana, R. Amendola, S. Chevalier, P. Piccardo, G. Caboche, M. Viviani, R. Molins and M. Sennour: J. Power Sources., 171(2007), 652.
[32] N. Shaigan, W. Qu, D. G. Ivey and W. Chen: J. Power Sources., 195(2010), 1529.
[33] K. A. Al-Hatab, M. Al-Bukhaiti and U. Krupp: Appl. Surf. Sci, 318(2014), 275.
[34] H. Ebrahimifar and M. Zandrahimi: Ionics., 18(2012), 615.
[35] B. Nikrooz, M. Zandrahimi and H. Ebrahimifar: J. Sol Gel Sci. Tech., 63(2012), 286.
[36] F.Saeedpur, M. Zandrahimi and H. Ebrahimifar: Corros. Sci., 153(2019), 200.
[37] S. Osgerby, K. Berriche-Bouhanek and H. Evans: Mater. Sci. and Eng. A., 412(2005), 182.